Cryst. Res. Technol. **42**, No. 11, 1117 – 1122 (2007) / **DOI** 10.1002/crat.200710935

Increased optical damage resistance of Zr:$LiNbO_3$ crystals

Liang Sun*[1], Fengyun Guo[1], Qiang Lv[1,4], Haitao Yu[3], Hongtao Li[1], Wei Cai[1], Yuheng Xu[2], and Liancheng Zhao[1]

[1] School of Materials Science and Engineering, Harbin Institute of Technology, Harbin, 150001, P. R. China
[2] Department of the applied chemistry, Harbin Institute of Technology, Harbin, 150001, P. R. China
[3] School of applied science, Harbin University of Science and Technology, Harbin, 150080, P. R. China
[4] Devision of Electronic Technology, Mudanjiang Medical College, Mudanjiang, 157011, P. R. China

Received 7 March 2007, revised 19 April 2007, accepted 26 April 2007
Published online 4 July 2007

Key words Czochralski methold, lithium compound, photo-refracitve materials.
PACS 42.70.Mp, 78.30.-j, 78.20.Ci

Zr: $LiNbO_3$ crystals has been grown. The crystal composition and phase are analyzed by X-ray diffration. The optical damage resistance ability of Zr: $LiNbO_3$ crystals is studied by the Sénarmont compensation method and the transmitted beam pattern distortion method. The saturated value of the birefringence change of 6 mol % Zr: $LiNbO_3$ crystal is 1.01×10^{-4}, which is seven times smaller than that of congruent pure $LiNbO_3$ crystal. The results of UV-Visible and IR absorption spectra of Zr: $LiNbO_3$ crystals powerfully confirm that the optical damage resistance threshold concentration of the Zr^{4+} ions doped in $LiNbO_3$ crystals is about 6 mol % in the melt.

1 Introduction

Lithium niobate ($LiNbO_3$) crystal being excellent piezoelectric, electric-optical, optical and nonlinear optical properties had widely used in applied optics [1, 2], however, the optical damage originated by light induced refractive index changes restricted its industrial application [3]. Adding optical damage resistance dopants (i.e. the ODRD) of 5.0 mol % MgO, 6.5 mol % ZnO, 3.5 mol % In_2O_3 or 3.5 mol % Sc_2O_3 or increasing the Li/Nb ratios allows to overcome the shortages [4~6]. Recently, it was found to that the optical damage of 4 mol % HfO_2 doped $LiNbO_3$ crystal was the similar with that of 5~6 mol % MgO doped $LiNbO_3$ crystal [7]. Dissimilar to Mg^{2+}, Zn^{2+}, In^{3+} and Sc^{3+}, Hf^{4+} is a tetravalent ion and has shown some interesting and significant influence on the photorefractive properties of Fe: $LiNbO_3$ crystals and the periodic structure of HfO_2 doped PPLN crystals [8, 9]. The Zr^{4+} ions are the same as the Hf^{4+} ions in chemical valence. More important, the Zr^{4+} and Hf^{4+} ions site at the one subgroup in Periodic System of Elements. We may presume that the Zr^{4+} ions should be being ability of the optical damage resistance in $LiNbO_3$ crystal. Due to the smaller ions radius of Zr^{4+} ions than Hf^{4+} ions, Zr: $LiNbO_3$ crystals are easier growth than Hf: $LiNbO_3$ crystals. So the Zr^{4+} ions should be more excellent than Hf^{4+} ions as the ODRD if it was being the strong optical damage resistance ability in $LiNbO_3$ crystals.

In the letter, Zr:$LiNbO_3$ crystals has been grown by the Czochralski technique with various ZrO_2 doped concentration of 2 mol%, 4 mol%, 6 mol% and 8 mol% in the melt, respectively. The optical damage resistance ability of Zr: $LiNbO_3$ crystals is studied by the Sénarmont compensation method and the transmitted beam pattern distortion method. The results show that the optical damage resistance ability of 6 mol% Zr: $LiNbO_3$ crystal is the similar with that of 5~6 mol % MgO doped $LiNbO_3$ crystal and 4 mol % HfO_2 doped $LiNbO_3$ crystal.

* Corresponding author: e-mail: myfuture2002.student@sina.com

2 Crystal growth and sample preparation

The starting materials used for crystal growth were Li_2CO_3 (4N purity), Nb_2O_5 (4N purity) and ZrO_2 (4N purity). The crystals investigated here were prepared by the Czochralski technique with the fixed Li/Nb ratio of 0.946 and the various ZrO_2 doped concentrations of 0mol%, 2 mol%, 4 mol%, 6 mol% and 8 mol% in the melt (marked as $1^{\#}$, $2^{\#}$, $3^{\#}$, $4^{\#}$ and $5^{\#}$, respectively), along the [001] direction using a diameter-controlled Czochralski apparatus. Two congruent doped 5 mol % Mg: $LiNbO_3$ crystal ($6^{\#}$) and 4 mol % Hf: $LiNbO_3$ crystal ($7^{\#}$) were grown for comparison. In order to grow good quality crystals, the following optimum growth conditions were selected: the temperature gradient above the melt was 25 K/mm, the pulling rate was 0.8 mm/h and the seed rotation rate was 25 rpm. After growth, the crystal was cooled down to room temperature at a speed of 80 K/h. The diameter of all the product crystals was about 30mm, with a length of about 40 mm. All the crystals poled at 1200°C with a current density of the 5 mA/cm^2. The crystals were cut into 8 mm×8 mm×2 mm (Z×X×Y) samples.

3 Experimental

The $1^{\#}$, $2^{\#}$, $3^{\#}$, $4^{\#}$ and $5^{\#}$ crystals were grinded into fine powders, and the powder structures and phase identification were done by X-ray Rigaku diffractometer D/max-24w with a graphite monochromator. The lattice parameters were calculated by the least-squares method. To measure the optical damage resistance ability of the Zr: $LiNbO_3$ crystals we used the Sénarmont compensation method [10]. The experimental setup for measurement of the change in optical birefringence was described by Fontana et al. [11]. A low power He-Ne laser (λ = 623.8 nm, 1.0 mW, 1.5 mm beam diameter) was used as a probe source, and an Ar^+-ion laser (λ = 488.0 nm, 1.5 mm beam diameter) with an incident power of 300 mW was used to induce optical damage. We could determine the change in the photorefractive-induced phase shift between the ordinary and extraoidinary components of the probe beam by measuring the analyzer's rotation angle needed for compensation. The change in the transmitted He-Ne laser radiation intensity was monitored with a photodetector as a function of time. The photo-induced birefringence change is linked to the space charge field E_{sc} generated by laser irradiation in an electro-optical process expressed as

$$\delta\Delta n = \frac{1}{2} n_e^3 r_c E_{sc}, \tag{1}$$

where $r_c = r_{33}-(n_o/n_e)r_{13}$ is the effective linear eletro-optic coefficient, which was recently shown to be strongly dependent on the crystal composition. Due to the photo-induced birefringence are fitted to first-order exponential time response function given by

$$\delta\Delta n = \Delta n_s[1-\exp(-t/\tau)], \tag{2}$$

where τ is the characteristic time of the Δn_s the saturated value of the birefringence change.

The optical damage resistance ability of Zr: $LiNbO_3$ crystals was also studied by the transmitted beam pattern distortion method [12]. Figure 1 showed the experimental set-up. The Ar^+-ion laser (λ= 488.0 nm) beam was focused by means of a convex lens of focal length *f* onto a crystal sample placed in the focal plane. The laser radiation was polarized parallel to the *c*-axis of the crystal. Optical damage was not induced in the crystal when the laser power intensity was low, and the pattern of the transmitted beam was round on the screen. When the laser intensity exceeded a certain value, optical damage generated within the crystal, and the pattern of the transmitted beam became elongated along the *c*-axis.

The unpolarized ultraviolet-Visibleible optical absorption spectra of the series of crystals were measured by a CARY2390 ultraviolet-Visibleible spectrophotometer at room temperature. The measurement range was from 200 to 800nm. The infrared transmittance was measured by a Fourier infrared spectrometer (Niconet-710, Nicolet, USA) at room temperature in the wavelength range of 400~4000 cm^{-1}.

4 Results and discussion

The lattice constants of all the samples with various doped Zr ions concentration are obtained from an X-ray Rigaku diffractometer D/max-24w with a graphite monochromator. As shown in table 1 and figure 2, all the

samples are in a single phase, but the local structure is modified by the incorporation of doped Zr ions. The c/a value of the $2^{\#}$ sample is higher than that of the $1^{\#}$ sample, which means the ZrO_2 dopant increases the value of c/a. With increasing the doped Zr ions concentration, the c/a value goes up continuously. The results suggest that the variation of the doped Zr ions concentration could affect the occupation of Zr^{+} ions in the LN crystal matrix. The position that the dopants occupy in the lattice of the LN crystal matrix is decided by the local chemical bonding state, the size and normal valence of atoms, and the chemical environment of the LN matrix according to the bond valence model (the BVM).

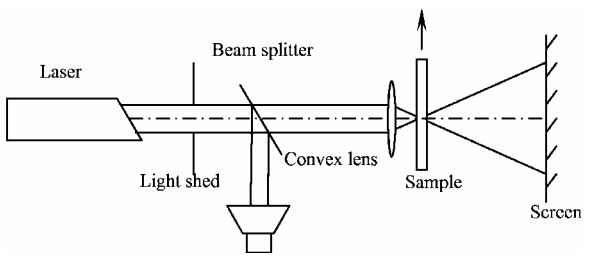

Fig. 1 Experimental setup for optical damage resistance measurements.

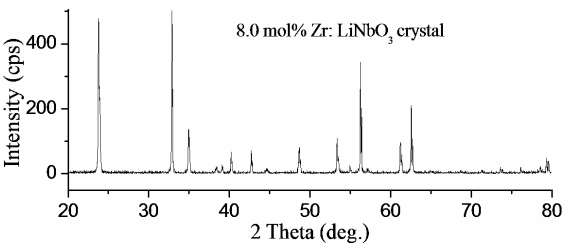

Fig. 2 X-ray powder diffraction patterns of 8.0 mol%Zr: $LiNbO_3$ crystal.

Table 1 Lattice constant of doped Zr: $LiNbO_3$ crystals with various doped Zr ions concentration.

Crystal (No.)	a/nm	b/nm	c/nm	c/a
$1^{\#}$	0.515223	0.515223	1.385145	2.6884
$2^{\#}$	0.515304	0.515304	1.386437	2.6905
$3^{\#}$	0.514987	0.514987	1.386214	2.6917
$4^{\#}$	0.514874	0.514874	1.386011	2.6919
$5^{\#}$	0.514801	0.514801	1.386411	2.6931

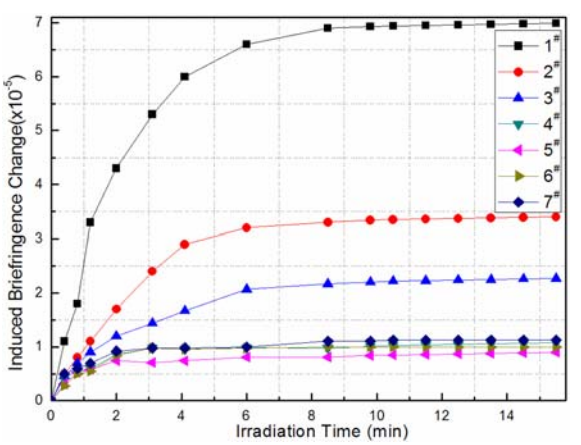

Fig. 3 Optically induced birefringence change of Zr, Mg and Hf doped $LiNbO_3$ crystals irradiated with an Ar^{+}-ion laser beam.

Figure 3 shows the optically induced change in the birefringence of Zr: $LiNbO_3$ crystals with various ZrO_2 doped versus irradiation time. The saturated change values in the birefringence of the crystals decrease with the increase of ZrO_2 doped concentration. In particularly, when the concentration of ZrO_2 doped exceeds 6 mol% in the melt, the decrease is very obvious. Table 2 summarizes the saturated value of the birefringence change of Zr: $LiNbO_3$ crystals with various Zr ions doped concentrations. The results indicate that the saturated value of the birefringence change of Zr: $LiNbO_3$ crystals can be reduced by the ZrO_2 doped. When the concentration of the ZrO_2 doped is 2 mol% in the melt (the $2^{\#}$ sample), the Δn_s value is 3.4×10^{-5}, which is more two times lower than that of congruent pure $LiNbO_3$ crystal. When the ZrO_2 doped concentration increases from 2 mol% to 4 mol%, the saturated value of the birefringence change is reduced to 2.2×10^{-5} (for the $3^{\#}$ sample). In particularly, the concentration of ZrO_2 doped reaches 6 mol % in the melt (the $4^{\#}$ sample), the saturated value of the birefringence change of Zr: $LiNbO_3$ crystal is abruptly reduced to 1.01×10^{-4}, which is seven times smaller than that of congruent pure $LiNbO_3$ crystal. To the crystals in which the doped concentrations of ZrO_2

are more than 6 mol% in the melt, the saturated values of the birefringence change are weakly reduced compared with that in the 6 mol% Zr: $LiNbO_3$ crystal. So we may infer that the Zr^{4+} ions optical damage resistance threshold in Zr: $LiNbO_3$ crystal should be about 6 mol% in the melt, which is confirmed by the results of UV-Visible and IR absorption spectra below. At the same time, the results show that the optical damage resistance ability of 6 mol% Zr: $LiNbO_3$ crystal is the similar with that of 5mol % MgO doped $LiNbO_3$ crystal and 4 mol % HfO_2 doped $LiNbO_3$ crystal.

Table 2 The saturated value of the birefringence change of Zr, Mg and Hf doped $LiNbO_3$ crystals.

Crystal (No.)	$1^{\#}$	$2^{\#}$	$3^{\#}$	$4^{\#}$	$5^{\#}$	$6^{\#}$	$7^{\#}$
Δn_s (10^{-5})	7.00	3.40	2.20	1.01	0.99	1.00	1.12

Figure 4 shows the distortion of the transmitted light spot when the samples are irradiated with the Ar-laser at the same power level. $LiNbO_3$ crystal ($1^{\#}$) shows a severe distortion along the c-axis in the beam (figure 4b). The 2 mol % Zr: $LiNbO_3$ crystal ($2^{\#}$) and 4 mol % Zr: $LiNbO_3$ crystal ($3^{\#}$) display slight distortion in the beam (figure 4c and d). The 6 mol % Zr: $LiNbO_3$ crystal ($4^{\#}$) and 8mol % Zr: $LiNbO_3$ crystals ($5^{\#}$) are found to be able to withstand the laser power density without noticeable distortion in the beam slight distorted in the beam (figure 4e and f).

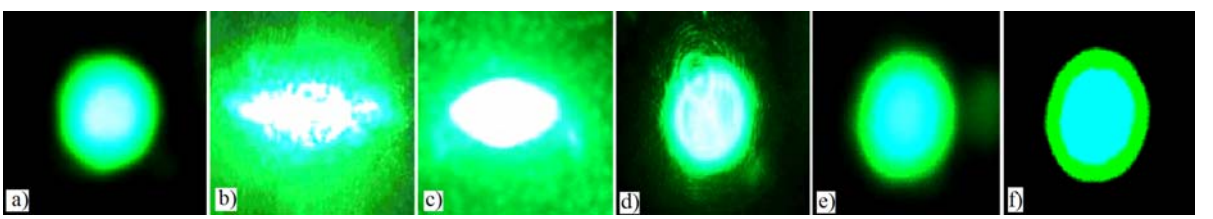

Fig. 4 Transmitted laser beam distortions with Ar-laser irradiation at steady state for equal irradiation times: (a) Ar-laser beam (no crystal); (b) undoped $LiNbO_3$; (c) 2 mol%Zr: $LiNbO_3$ crystal; (d) 4 mol%Zr: $LiNbO_3$ crystal; (e) 6 mol%Zr: $LiNbO_3$ crystal; (f) 8 mol%Zr: $LiNbO_3$ crystal.

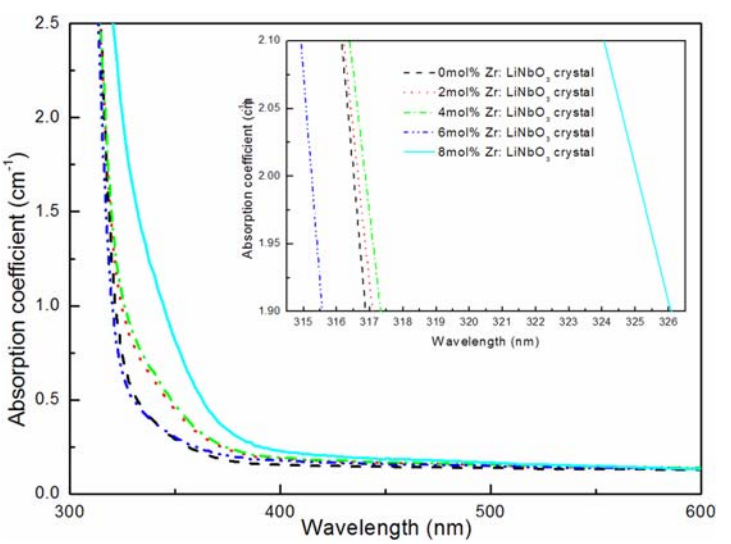

Fig. 5 UV-Visible absorption spectra of the Zr:$LiNbO_3$ crystals.

Figure 5 shows the unpolaried UV-Visible absorption spectra of the Zr: $LiNbO_3$ crystals grown from melts with the various doped Zr ions doped concentration at room temperature. The absorption edges of the $LiNbO_3$ crystals had been used to determine the composition and defects, especially sensitive to the optical damage resistance dopants in $LiNbO_3$ crystals [13-15]. The inset of figure 5 is the partial enlarged figure, which shows the absorption edge positions of crystals with the various ZrO_2 doped concentration in the melt. When the ZrO_2 doped concentrations were below or above 6 mol% in the melt, the absorption edges of Zr: $LiNbO_3$ crystals red-shift compared with undoped $LiNbO_3$ crystal with increase in the ZrO_2 doped concentration. For the

6 mol% Zr: $LiNbO_3$ crystals, the absorption edges obviously blue-shift compared with undoped $LiNbO_3$ crystal. The obviously blue-shifting of the absorption edge for the 6 mol% Zr: $LiNbO_3$ crystal powerfully verifies the existence of the Zr^{4+} ions optical damage resistance threshold concentration in Zr: $LiNbO_3$ crystals according to [13-15]. The absorption edge position of the samples can also be compared by the wavelength where the absorption coefficient has a certain value. In this work, we use as a criterion the wavelength at the absorption coefficient α=20cm^{-1} as introduced by Földvári et al. [16,17]. In the $1^{\#}$, $2^{\#}$, $3^{\#}$, $4^{\#}$ and $5^{\#}$ crystals, the absorption edge position are located at 316.6 nm, 316.8 nm, 317.0 nm, 315.2 nm and 325.1 nm, respectively.

Figure 6 shows the IR optical transmission spectra of Zr: $LiNbO_3$ crystals corresponding to the various ZrO_2 doped concentrations in the melt. The OH^- vibration bands of all samples are narrow, and their main peaks are located at 3483 cm^{-1}, 3484 cm^{-1}, 3489 cm^{-1} and 3489 cm^{-1}, corresponding to the $2^{\#}$, $3^{\#}$, $4^{\#}$ and $5^{\#}$ crystals, respectively. We may find that the red-shift of the peak at 3489 cm^{-1} in the 6 mol% Zr: $LiNbO_3$ crystals is about 6 cm^{-1} relative to the peak at 3483 cm^{-1} in the weakly doped Zr: $LiNbO_3$ crystals, which further confirms the 6 mol% doped concentration in the melt is the Zr^{4+} ions optical damage resistance threshold concentration in $LiNbO_3$ crystal. The marker OH^--associated vibrational peak of the ZrO_2 optical damage resistance threshold in $LiNbO_3$ crystal is located at 3489 cm^{-1}, which may represent the $(Zr_{Nb})^-$ defect structure around a OH^- ion, i.e. the $(Zr_{Nb})^-$-OH^- defect centra.

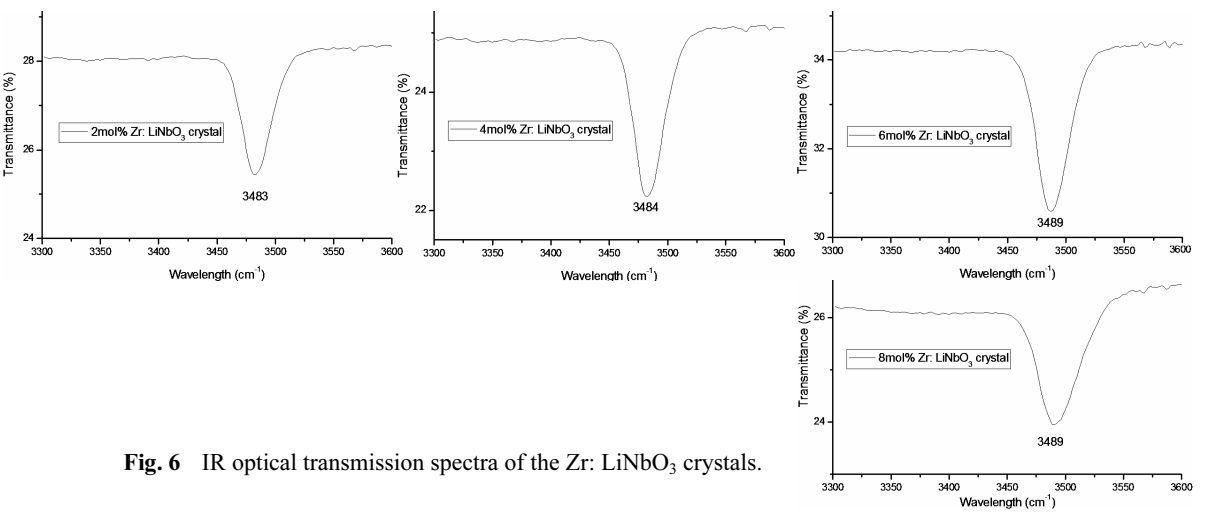

Fig. 6 IR optical transmission spectra of the Zr: $LiNbO_3$ crystals.

5 Conclusions

The optical damage resistance ability of Zr: $LiNbO_3$ crystals has been investigated by the Sénarmont compensation method and the transmitted beam pattern distortion method. The results show the optical damage resistance of Zr: $LiNbO_3$ crystals are greatly enhanced compared with that of undoped $LiNbO_3$ crystal. In particular, The saturated value of the birefringence change of 6 mol % Zr: $LiNbO_3$ crystal is 1.01×10^{-4}, which is seventh times smaller than that of congruent pure $LiNbO_3$ crystal. The 6 mol% ZrO_2 doped concentration is thought as the Zr^{4+} ions optical damage resistance threshold concentration in Zr: $LiNbO_3$ crystals, which is confirmed by the results of the UV-Visible and IR absorption spectra. The absorption edges of the 6 mol% Zr: $LiNbO_3$ crystals obviously blue-shift compared with undoped $LiNbO_3$ crystal. The marker OH^--associated vibrational peak of the ZrO_2 optical damage resistance threshold concentration is located at about 3489 cm^{-1} corresponding to the $(Zr_{Nb})^-$-OH^- defect centra.

References

[1] H. J. Coufal, D. Psaltis, and G. T. Sincerbox "Holographic Data Storage", Springer, Berlin, 2000.
[2] P. Boffi, D. Piccinin, and M. C. Ubaldi (Eds.), "Infrared Holography for Optical Communications", Springer, Berlin, 2003.

[3] A. Ashkin, G. Boyd, J. Dziedzic, R. Smith, A. Ballman, J. Levinstein, and K. Nassau, Appl. Phys. Lett. **9**, 72 (1996).
[4] T. R. Volk, V. I. Pryalkin, and N. M. Rubinina, Opt. Lett. **15**, 996 (1990).
[5] Y. F. Kong, J. K. Wen, and H. F.Wang, Appl. Phys. Lett. **66**, 280 (1995).
[6] J. K. Yamamoto, K. Kitamura, N. Iyi, S. Kimura, Y. Furukawa, and M. Sato, Appl. Phys. Lett. **61**, 2156 (1992).
[7] L. Razzari, P. Minzioni, I. Cristiani, V. Degiorgio, and E. P. Kokanyan, Appl. Phys. Lett. **86**, 131914 (2005).
[8] S. Li, S. Liu, Y. Kong, J. Xu, and G. Zhang, Appl. Phys. Lett. **89**, 101126 (2006).
[9] E.P. Kokanyan, L. Razzari, I. Critiani, V. Degiorgio, and J. B. Gruber, Appl. Phys. Lett. **84**, 1881 (2004).
[10] Y. Furukawa, M. Sato, K. Kitamura, Y. Yajima, and M. Minakata, J. Appl. Phys. **72**, 3250 (1992).
[11] M. Fontana, K. Chah, M. Aillerie, R. Mouras, and P. Bourson, Opt. Mater. **16**, 111 (2001).
[12] X. H. Zhen, W. S. Xu, C. Z. Zhao, L. C. Zhao, and Y. H. Xu, Cryst. Res. Technol. **37**, 976 (2002).
[13] Q. Li, X. H. Zhen, and L. Wang, J. Cryst. Growth **284**, 273 (2005).
[14] S. Li, S. Liu, and Y. Kong, J. Phys.: Cond. Matt. **18**, 3533 (2006).
[15] X. H. Zhen, W. S. Xu, and Q. Li, J. Cryst. Growth. **271**, 472 (2004).
[16] I. Földvári, K. Polgár, R. Voszka, and R. N. Balasanyan, Cryst. Res. Technol. **19**, 1659 (1984).
[17] K. Polgár, Á. Péter, L. Kovács, G. Corradi, and Z. Szaller, J. Cryst. Growth **177**, 211 (1997).

